A Super Low-Noise 0.1 μm *T*-Gate InAlAs–InGaAs–InP HEMT

K. H. G. Duh, P. C. Chao, S. M. J. Liu, P. Ho, M. Y. Kao, and J. M. Ballingall

***Abstract*—0.1 μm *T*-gate InAlAs–InGaAs–InP HEMT's developed in our laboratory have exhibited state-of-the-art noise and gain performance well up to 100 GHz. Minimum noise figures of 0.8 and 1.2 dB with gains of 8.9 and 7.2 dB have been measured at 60 and 94 GHz, respectively. The *W*-band low-noise result is the best noise performance ever observed for any microwave transistors. A high performance *W*-Band three-stage amplifier has been built using these devices: noise figures between 3.2 dB–3.5 dB with gain of 17.5 ± 0.4 dB from 91 to 96 GHz. 6 dB improvement in the 1 dB compression characteristic of the amplifier has been achieved with a GaAs pseudomorphic HEMT in the third stage.**

I. Introduction

Significant progress has been made recently in the GaAs-based and InP-based HEMT technology [1]–[4]. HEMT's with a single quantum well-active channel composed of InGaAs grown on GaAs and InP substrates are establishing new standards of performance well up to 94 GHz. Advantages of *W*-band operations include large absolute bandwidth, high resolution, small aperture area, lightweight, and ECM/clutter resistance, have drawn the attention for the applications in the areas of communication links, seekers for weapons, tank/ship defense, radiometry, and commercial anti-collision radars. In this paper, we report record low noise and gain performance of 0.1 μm gate-length InAlAs/InGaAs/InP HEMT's, show the millimeter-wave on-wafer noise parameter characterization technique, and present the high performance *W*-band amplifier results.

II. InAlAs–InGaAs–InP HEMT's

The devices were fabricated on selectively doped InAlAs–InGaAs heterostructures grown by MBE on InP substrates [5], [6]. The InAlAs–InGaAs–InP lattice-matched HEMT has 53% InAs in the channel. The higher InAlAs–InGaAs conduction band discontinuity and low energy bandgap of the $In_{.53}Ga_{.47}As$ channel offer high electron sheet charge density and better carrier confinement in the channel, resulting in superior electron transport to achieve higher transconductance, g_m, current gain cutoff frequency (f_t), and lower noise figure than GaAs-based pseudomorphic HEMT's (pHEMT). The concept of planar doping has been implemented in this heterostructure to enhance the two-dimensional electron gas (2-DEG) density for the reduction of series resistance and increase of current density. The 0.1 μm T-gate profile is obtained by tri-layer PMMA-P (MMA-MAA)–PMMA electron beam resists. The gate resistance is approximately 200 Ω/mm, which is similar to that of our 0.15 μm *T*-gate devices. Typical extrinsic g_m is 1200 mS/mm. Table I displays the room temperature noise and gain performance of the 0.1 μm InP-based HEMT's at 60 and 94 GHz. Minimum noise figures of 0.8 and 1.2 dB with associated gains of 8.9 and 7.2 dB have been measured at 60 and 94 GHz for device widths of 50 μm and 30 μm, respectively. The test fixture correction for device noise figures is 0.4 dB at 60 GHz, and 0.8 dB at 94 GHz. The correction is based upon the minimum end-to-end loss of waveguide-to-microstrip transition including matching circuits with better than 20 dB return loss across the test bands. The *W*-band measured results have been cross-checked by other established laboratories. All measured noise figures agreed to within 0.3 dB range. Drain voltage at low noise condition is typically 1.0 Volt. The comparison of the 1-dB compression characteristics for InP-based and GaAs-based devices is shown in Fig. 1. The lower 1 dB compression point in the InP-based HEMTs is due to its inferior gate characteristic and low drain voltage.

TABLE I
Noise and Gain Performance of 0.1μm *T*-Gate InAlAs–InGaAs–InP HEMT's at Room Temperature

Freq. (GHz)	F_{min} (dB)	G_a (dB)	$F\infty$* (dB)
60	0.8	8.9	0.91
94	1.2	7.2	1.44

Note:

$$F\infty = F + \frac{F-1}{G} + \frac{F-1}{G^2} + \cdots$$

$$= 1 + \frac{F-1}{1-1/G}$$

*$F\infty$ is defined as the noise figure of an infinite chain of cascaded single-stage amplifiers. It is a useful figure of merit for circuit design that closely approximates the noise figure attainable in a multistage amplifier, neglecting circuit losses.

III. On-Wafer RF Characterization

On-wafer RF characterization has recently received a lot of attention due to the advantages of accurate parameter extraction, rapid performance feedback, and cost effective testing. Unfortunately for the noise parameter measurement, commercial equipment is only available up to 26 GHz. We have developed 6–40 GHz on-wafer noise parameter measurement capability to provide critical design information for the low noise amplifiers (LNA). It is based on the principle of

Manuscript received January 23, 1991.
The authors are with the Electronics Laboratory, General Electric Company, P.O. Box 4840, Syracuse, NY 13221-4840.
IEEE Log Number 9144464.

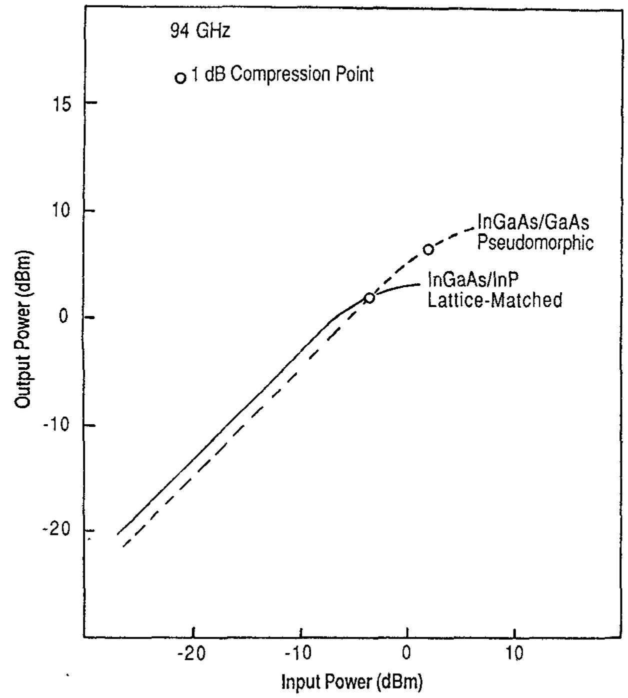

Fig. 1. Device gain compression characteristics of InP HEMT and GaAs pseudomorphic HEMT for gate width of 50 μm at 94 GHz.

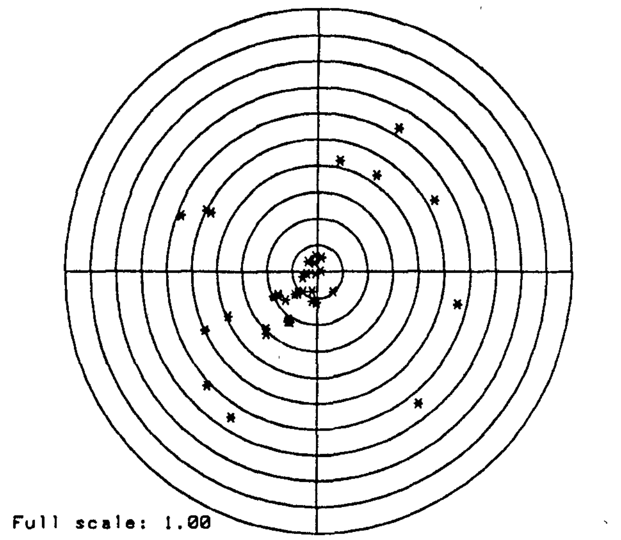

Fig. 2. Available impedance states generated at the probe tip at 40 GHz. Full scale of polar display is 1.0.

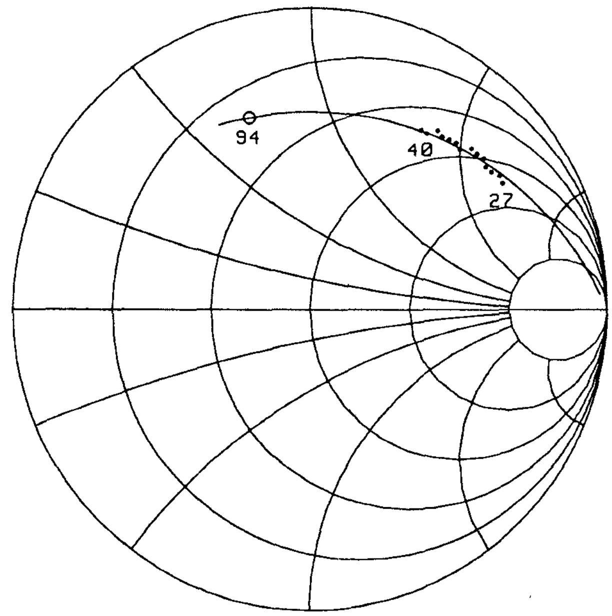

Fig. 3. Optimum source impedance contour of the InP HEMT: Data points from 27 to 40 GHz are from measured results and the 94 GHz point is extrapolated from low frequencies.

combining network measurement using a vector network analyzer (HP8510B) and noise power measurement using a noise figure meter (HP8970). A number of room temperature impedance states plus an elevated noise temperature state are presented to the input of the device while the output noise power are measured and the associated noise figure are deduced. The four noise parameters can then be determined [7], [8].

Specially constructed solenoid driven mechanical switches are used to alternate between the connection from the wafer probers to the network analyzer and that to the noise figure meter. The mechanical switches also connect combinations of coaxial delay lines and attenuators so that a number of impedance states can be created. Since these are passive devices kept at room temperature, only room temperature Johnson noise is associated with these impedance states. A precision solid-state diode noise source is used for the elevated temperature impedance state. Fig. 2 shows the reflection coefficient of the available impedance states at the probe tip at 40 GHz. Due to the use of low loss probes (Tektronix TMP 9600 series) and low loss, low reflection mechanical switches, the impedance states are well spread out in magnitude and phase. The spreading of the impedance states allows for accurate determination of the noise parameters. Special effort in constructing the switches produced highly accurate *S*-parameter measurement and noise measurement results. The switches are pretested for high repeatability. At 40 GHz, the largest excursion from the average transmission loss of the switches is less than 0.01 dB, while that of the phase is less than 0.3°.

S-parameter calibration standards made on InP wafer includes open, short, load and through line. Extended short and open are also used for verifying the calibration. A set of waveguide standard is used for calibrating the waveguide port that connects the standard noise source. The loss of the network between the noise source and the probe tip is accurately determined. Fig. 3 illustrates the position of the optimum source impedance of the InP HEMT. The data points from 27 to 40 GHz are from measured results; based on our noise model for the device, the 94 GHz data is extrapolated and shown.

IV. Results

The LNA uses 30-μm gate-width devices for the first and second stages. This width is selected based on the analysis of the noise matching at the input of device. Frequency response of R_{opt} (optimum resistance of noise match) for various

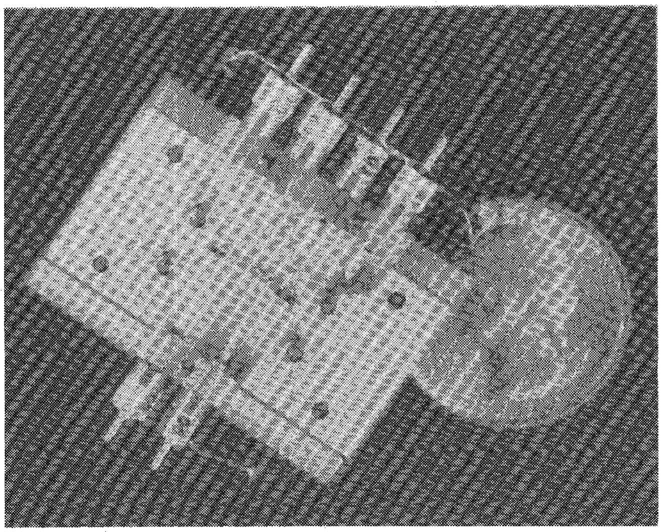

Fig. 4. Photograph of *W*-band three-stage low-noise amplifier with the cover removed.

width of HEMT's were measured to select the optimum width for the *W*-band application. It concludes that 30 μm will provide good range of impedance for the circuit design. We use 50 μm GaAs-based passivated pHEMT device (typical breakdown voltage of 8-9 V) as output stage to have good output VSWR and large power handling capability to achieve high dynamic range.

The input and output ports of the LNA utilize a broad-band *E*-field probe circuit for the waveguide to microstrip transitions. A photograph of a three-stage LNA with the cover plate removed is shown in Fig. 4. The edge-coupled symmetric microstrip transmission line structure was selected to provide low-loss DC blocking. It was designed as a bandpass filter to enhance out of band stability. The matching circuits based on the calculated *W*-band noise parameters and equivalent circuit model were fabricated on a 5 mil quartz substrate. Fig. 5 shows the performance of the 3-stage LNA measured from input waveguide flange to output waveguide flange. Noise figures between 3.2 dB to 3.5 dB have been measured. The flat gain response of the amplifier is 17.5 ± 0.4 dB from 91 to 96 GHz. Using a GaAs pHEMT as the third-stage, the 1 dB compression point of this LNA is 0 dBm output power, which is approximately 6 dB improvement compared with using all InP HEMT devices. The input return loss is better than 7 dB for the LNA across the test band.

V. Conclusion

We have demonstrated state-of-the-art low noise performance from our 0.1 μm *T*-gate InAlAs-InGaAs-InP HEMT's. Minimum noise figures of 0.8 and 1.2 dB with gains of 8.9 and 7.2 dB have been measured at 60 and 94 GHz, respectively. With the accurate millimeter-wave noise parameter measurement capability we are able to combine the advantages of InP-based and GaAs-based devices to demonstrate a super low-noise and high-dynamic range three-stage LNA. It gives noise figures of 3.2 dB-3.5 dB with the flat gain response of 17.5 ± 0.4 dB from 91 to 96 GHz. The results clearly show the great potential of 0.1 μm gate-length InP HEMT's for high performance millimeter-wave low-noise receiver applications.

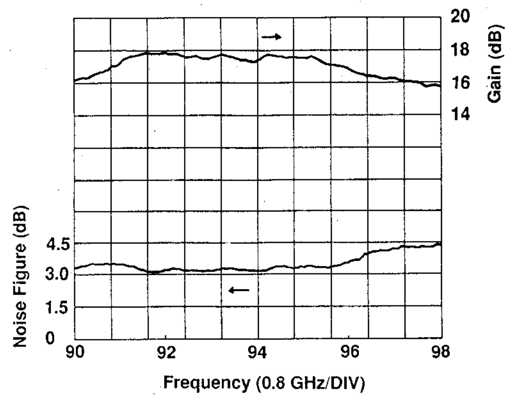

Fig. 5. Gain and noise performance of *W*-band three-stage HEMT low-noise amplifier.

References

[1] K. H. G. Duh, P. C. Chao, P. Ho, A. Tessmer, S. M. J. Liu, M. Y. Kao, P. M. Smith, and J. M. Ballingall, "*W*-band InGaAs HEMT low-noise amplifiers," *IEEE MTT-S Dig.*, pp. 595-598, May 1990.

[2] K. L. Tan, R. M. Dia, D. C. Streit, T. Lin, T. Q. Trinh, A. C. Han, P. H. Liu, P. M. D. Chow, and H. C. Yen, "94-GHz 0.1-μm *T*-gate low-noise pseudomorphic InGaAs HEMT's," *IEEE Electron Device Lett.*, vol. 11, no. 12, pp. 585-587, Dec. 1990.

[3] Y. Mimino, K. Joshin, S. Ohmura, and Y. Hirachi, "Noise performance of AlGaAs-InGaAs HEMT's with 0.15 μm *T*-shaped W-Six gate at cryogenic temperature," in *3rd Asia-Pacific Microwave Conf. Proc.*, Sept. 1990, pp. 645-648.

[4] L. D. Nguyen, L. M. Jelloian, M. Thompson, and M. Lui, "Fabrication of a 80 nm self-aligned *T*-gate AlInAs-GaInAs HEMT," *1990 IEEE IEDM*, San Francisco, CA, Paper 19.1, Dec. 1990.

[5] P. Ho, P. C. Chao, K. H. G. Duh, A. A. Jabra, J. M. Ballingall, and P. M. Smith, "Extremely high gain, low-noise InAlAs-InGaAs HEMT grown by molecular beam epitaxy," *1988 IEEE IEDM*, San Francisco, CA, Paper 8.5, Dec. 1988.

[6] P. M. Smith, P. C. Chao, P. Ho, K. H. G. Duh, M. Y. Kao, J. M. Ballingall, S. T. Allen, and A. Tessmer, "Microwave InAlAs-InGaAs-InP HEMT's: Status and applications," *2nd Int. Conf. Indium Phosphide and Related Materials*, Denver, CO, Apr. 1990 pp. 39-43.

[7] R. Q. Lang, "The determination of device noise parameters," *Proc. IEEE*, vol. 57, pp. 1462-1462, Aug. 1969.

[8] A. C. Davidson, B. W. Leake, and E. Strid, "Accuracy improvements in microwave noise parameter measurements," *IEEE Trans. Microwave Theory Tech.*, vol. 37, pp. 1973-1978, Dec. 1989.